[6] K. M. Chen and S. Rukspollmaung, "Hyperthermia in animal and human bodies induced by EM fields," *J. Bioeng.*, vol. 1, pp. 531–539, 1977.
[7] D. Livesay and K. M. Chen, "Electromagnetic field inside arbitrary shaped biological bodies," *IEEE Trans. Microwave Theory Tech.*, vol. MTT-22, pp. 1273–1280, Dec. 1974.
[8] J. VanBladel, "Some remarks on Green's dyadic for infinite space," *IRE Trans. Antenna Propagat.*, vol. AP-9, pp. 563–566, Nov. 1961.
[9] R. F. Harrington, *Field Computation by Moment Methods.* New York: Macmillan, 1968, ch. 1.
[10] M. K. Hessary, "Local heating of biological bodies with HF electric and magnetic fields," Ph.D. dissertation, Michigan State Univ. East Lansing, 1982.
[11] K. M. Chen, S. Rukspollmaung, and D. P. Nyquist, "Measurement of induced electric field in a phantom model of man," *Radio Sci.*, vol. 17, no. 5(S), pp. 49S-59S, Sept.–Oct. 1982.

Manochehr Kamyab Hessary (M'82) was born in 1947 in Iran. He received B.S. and M.S. degrees, both in physics, from the University of Tehran, Iran, in 1970 and 1976, and Ph.D. in electrical engineering from Michigan State University, East Lansing, in 1982. He returned to Iran in 1983.

Kun-Mu Chen (SM '64–F'76) was born in Taipei, Taiwan, China, on February 3, 1933. He received the B.S.E.E. degree from the National Taiwan University, Taipei, Taiwan, in 1955, and the M.S. and Ph.D. degrees in applied physics from Harvard University, Cambridge, MA, in 1958 and 1960, respectively.

While at Harvard University, he held the C. T. Loo and the Gordon McKay Fellowships. From 1956 to 1957, he was a Teaching Assistant at the National Taiwan University, and from 1959 to 1960 he was a Research Assistant and Teaching Fellow at Harvard University. From 1960 to 1964, he was associated with the Radiation Laboratory, University of Michigan, Ann Arbor, where he was engaged in studies of electromagnetic theory and plasma. In 1962, while on leave from the University of Michigan, he was a Visiting Professor of Electronics at Chao-Tung University, Taiwan. Since 1964, he has been with Michigan State University, East Lansing, first as Associate Professor of Electrical Engineering, and since 1967 as Professor of Electrical Engineering. From 1968 to 1973, he was the Director of the Electrical Engineering program of the Department of Electrical Engineering and Systems Science. He has published numerous papers on electromagnetic radiation and scattering, plasmas, and the interaction of electromagnetic radiation with biological systems.

Dr. Chen is a fellow of the American Association for the Advancement of Science, a member of U.S. Commissions A, B, and C of the International Scientific Radio Union, Sigma Xi, Phi-Kappa-Phi and Tau-Beta-Pi. He is the recipient of the Distinguished Faculty Award from Michigan State University in 1976. He is also the recipient of the Excellent Achievement Award from the Taiwanese American Foundation in 1983.

Microwave Modeling of Rectangular Tunnels

BENJAMIN JACARD AND OSCAR MALDONADO, MEMBER, IEEE

Abstract—**Natural propagation of electromagnetic waves in rectangular tunnels is investigated experimentally at microwave frequencies (1–10 GHz) using a tunnel model of reduced dimensions made of a lossy mixture of sand, water, and salt. The experimental results for the propagation constant of the low-order modes agree satisfactorily with theoretical predictions. Practical applications of the experimental technique are discussed.**

I. Introduction

To DESIGN IMPROVED communication systems in mine and road tunnels it is necessary to understand the mechanisms of natural propagation. This is not always possible due to difficulties in finding suitable theories for real tunnels. Furthermore, there is not enough experimental data on tunnels to verify the approximate theories proposed. Reliable measurements in real tunnels are difficult and costly due to instrumentation and access problems. For these reasons we propose the use of scale-modeling techniques using tunnel models made from a mixture of sand, water, and salt. This mixture has been previously used for modeling real ground at microwave frequencies [1], [2].

In this paper, experimental results are presented for propagation in a microwave-modeled rectangular tunnel. Results compare satisfactorily with published theory [3], suggesting that this modeling technique could be successfully used for investigating experimentally the propagation in other tunnels of more complex geometry where the theoretical approach would be difficult to apply.

Manuscript received April 12, 1983; revised January 10, 1984. This work was supported by the University of Chile under Grant DDI 1448-8323.

The authors are with the Department of Electrical Engineering, University of Chile, Santiago, Chile.

II. Theory of Propagation

An exact analytical solution for propagation in a rectangular tunnel is not possible because of the difficulty in

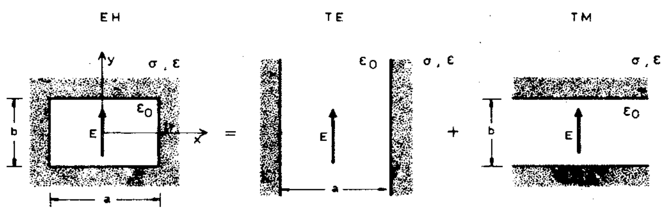

Fig. 1. Geometry of waveguides.

matching the boundary conditions [4]. An approximate theory has been recently proposed [3]. The propagation constant γ of a general EH mode in a rectangular tunnel of width a and height b is given by

$$\gamma^2 = k_x^2 + k_y^2 - k_0^2 \tag{1}$$

where k_x and k_y are complex transverse wavenumbers and k_0 is the free-space wavenumber.

Considering, for example, only vertically polarized waves, it has been shown [3] that k_x and k_y can be given by the transverse wavenumbers of two infinite slot waveguides of slot widths a and b, respectively, one supporting a TE mode and the other a TM mode as shown in Fig. 1.

The boundary value problem of the slot waveguides with lossy walls is easily solved using a standard procedure [5], [6]. It will be assumed that the source of the fields in the rectangular tunnel excites only vertically polarized waves and that these are even about $x = 0$ and $y = 0$; therefore, the same conditions will apply to the E field in the slot waveguides depicted in Fig. 1.

With the above symmetry considerations, the electromagnetic boundary conditions yield the following transcendental equations for k_x and k_y:

$$k_x \tan(k_x a/2) = \left(k_0^2(1-\tilde{\epsilon}_r) - k_x^2\right)^{1/2} \tag{2}$$

$$k_y \tan(k_y b/2) = \left(k_0^2(1-\tilde{\epsilon}_r) - k_y^2\right)^{1/2} / \tilde{\epsilon}_r \tag{3}$$

where $\tilde{\epsilon}_r$ is the complex relative permittivity of the walls ($\tilde{\epsilon}_r = [\epsilon - j(\sigma/\omega)]/\epsilon_0$).

First estimates for the roots k_x and k_y of (2) and (3) may be taken from the transverse wavenumbers of odd TE modes (i.e., TE_{10}, $TE_{30}, \cdots, TE_{n0}$) and even TM modes (i.e., $TM_{00}, TM_{02}, \cdots, TM_{0m}$) in perfectly conducting slot waveguides of widths a and b, respectively. Once the transverse wavenumbers are determined, the propagation constant of a natural mode EH_{nm} will be given by (1).

III. Experimental Model

The experimental model of a tunnel was built with a mixture of sand, 18-percent water, and 2-percent salt (weight percentages relative to the weight of the sand) which at 9.3 GHz gives approximately a relative permittivity $\epsilon_r = 9.3$ and a loss tangent $\tan\delta = 0.6$ [2]. The tunnel was formed by surrounding a polyfoam slab with this mixture. The slab had dimensions 0.08 m×0.05 m×2 m and very low relative permittivity ($\epsilon_r \approx 1.03$); it was placed for practical reasons over an aluminum plate, as illustrated in Fig. 2. The resulting tunnel with its image had a cross section $a \times b$ with $a = 0.08$ m and $b = 0.10$ m, which may

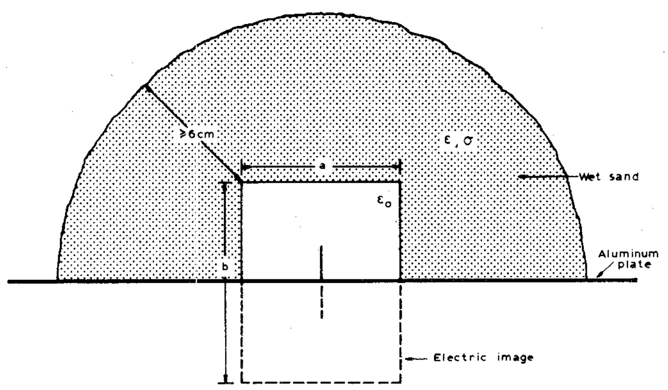

Fig. 2. Tunnel model geometry. $a = 8$ cm, $b = 10$ cm.

be taken to represent the Lanaye tunnel reported by Deryck [7] using a scaling factor of 50. Although the conductivity of this tunnel (10 mS/m at 30 MHz) was not properly scaled in the model in order to simulate an adequate electrical wall thickness, we expect to obtain from the model, in the band 1–10 GHz, similar propagation characteristics to those found in the real tunnel in the band 20–200 MHz.

The tunnel model was fed, 0.25 m from one end, by a monopole (1.75-cm height) vertically protruding at the center of the tunnel through the aluminum plate (Fig. 2). In this way, only vertically polarized waves of even symmetry were excited.

The relative amplitude and phase of the field inside the tunnel were measured on an HP 8410A Network Analyzer connected to a sliding vertical monopole probe (8.2-mm height) on the tunnel axis. The monopole and its feeding coaxial cable (2.5-mm diameter) lay on the aluminum plate and were moved by means of a string and pulley mechanism. The probe position was measured by an HP 7035B X–Y Recorder using as its reference a linear potentiometer formed by a resistive wire outside the tunnel and a sliding contact pulled by the string.

For convenience, the height of the monopole probes was not varied with frequency since we were interested only in relative amplitude and phase field measurements leading to the evaluation of the propagation constant of the modes.

IV. Measuring Techniques

The attenuation constant α of a propagating mode can be obtained from a plot of field strength in decibels against distance along the tunnel. The attenuation in decibels per meter will be given by the slope of the nearly straight line appearing in the plot when a single mode predominates. A beat pattern will indicate the presence of two or more modes propagating simultaneously, and the identification of the modes will be more involved. When two modes propagate with similar amplitudes and different phase constants β_1 and β_2, a regular beat pattern will be obtained, providing the necessary information for the calculation of the propagation constants of both modes, as shown in the Appendix.

In a similar manner, the phase constant β can be obtained by plotting the relative phase of the field against

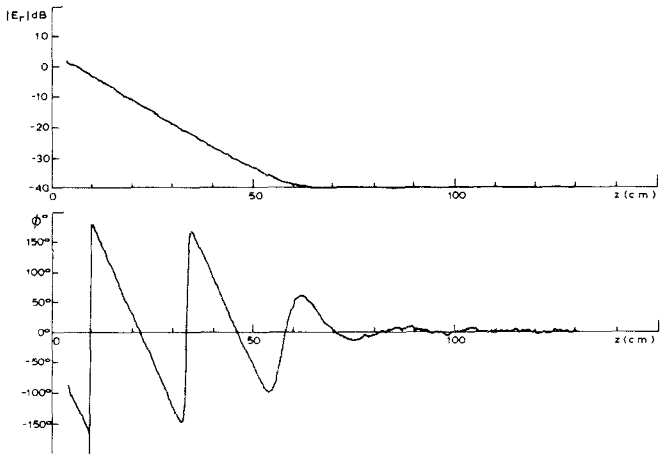

Fig. 3. Relative amplitude and phase distributions at 2.0 GHz.

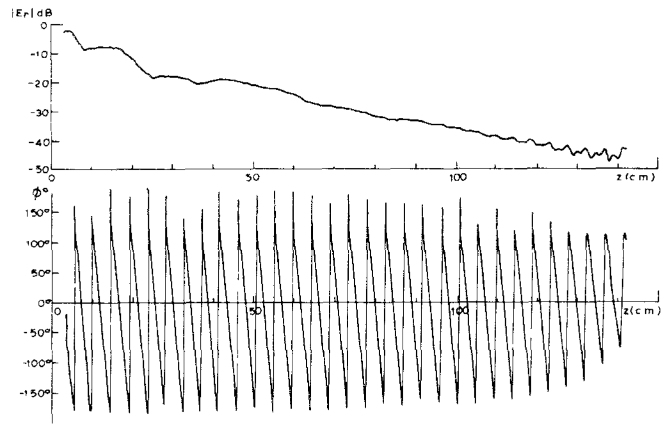

Fig. 5. Relative amplitude and phase distributions at 7.0 GHz.

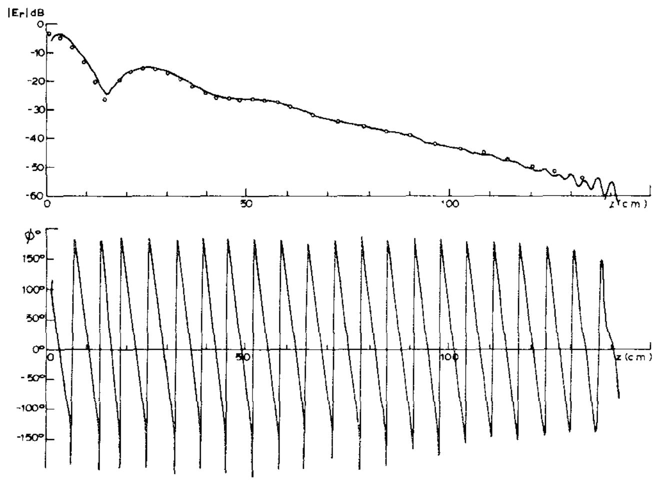

Fig. 4. Relative amplitude and phase distributions at 5.0 GHz.

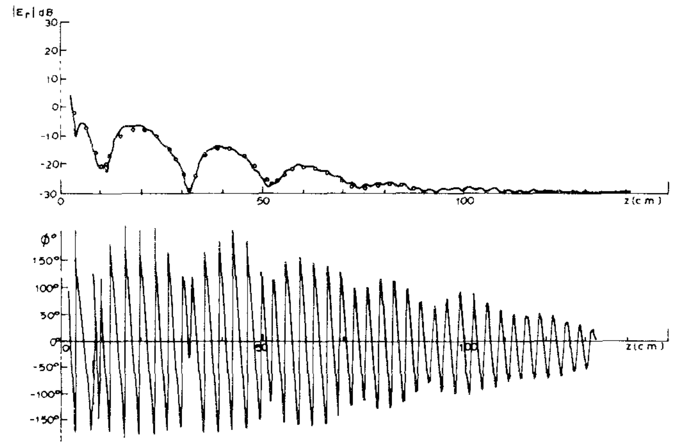

Fig. 6. Relative amplitude and phase distributions at 9.5 GHz.

distance along the tunnel. If only one mode propagates, the plot will consist of nearly straight line segments with well-defined slopes from which the phase constant can be determined. When two modes propagate, the beat wavelength λ_b of the amplitude pattern is easily measured and may be useful to identify the phase constant of one of the modes provided the phase constant of the other is already known (e.g., from the phase distribution far from the tunnel feed) since $\lambda_b = 2\pi/(\beta_1 - \beta_2)$.

V. Experimental Results

Typical relative amplitude and phase distributions along the tunnel model outlined in Section III are illustrated in Figs. 3, 4, 5, and 6 for frequencies 2.0, 5.0, 7.0, and 9.5 GHz, respectively. Between 1 and 3 GHz, only one mode was detected and its propagation constant was easily determined from the amplitude and phase distributions (see Fig. 3). In the band from 3 to 6 GHz, two-mode interference patterns were clearly obtained, as shown in Fig. 4.

From 6 to 9.0-GHz irregular amplitude distributions were obtained, and this is attributed to the interference of more than two propagating modes. Only at 7.0 GHz could one of the modes be identified due to its predominance far from the feeding end of the tunnel (see Fig. 5).

At 9.5 GHz, again a regular interference pattern was obtained (see Fig. 6), permitting the identification of the propagating modes with the procedure outlined in the Appendix.

TABLE I
Mode Parameters

	MODE 1			MODE 2		
FREQUENCY in GHz	RELATIVE AMPLITUDE	α in Np/m	β in rd/m	RELATIVE AMPLITUDE	α in Np/m	β in rd/m
1.00	1.00	22.5				
1.25	1.00	19.8				
1.60	1.00	15.8	16.3			
1.70	1.00	12.6	18.7			
2.00	1.00	8.5	26.4			
2.50	1.00	6.3	41.3			
3.16	1.00	5.0	56.2			
3.98	1.00	4.2	74.7	0.63	11.2	43.2
5.00	1.00	3.2	94.3	0.78	8.2	72.2
7.00	—	3.0	134.9	—	—	—
9.50	0.28	2.6	176.7	1.00	5.2	146.7

Experimental values of the propagation constant and relative amplitude of the modes identified in the band 1–10 GHz are included in Table I. In order to test the consistency of the values obtained from interference patterns (using four points), they have been used to synthesize the complete amplitude distribution along the tunnel by means of (A2) in the Appendix. Satisfactory agreement with the experimental distribution was obtained as shown in Figs. 4 and 6, (where the synthesized patterns are represented by dots), thus confirming the predominance of two propagating modes.

VI. Discussion of Results

Theoretical predictions for the propagation constant of the natural modes in the scale model can be obtained applying the method outlined in Section II to an equivalent tunnel of 8-cm width and 10-cm height with its four walls having the same electrical parameters and excited by a centered vertical dipole. For simplicity, the electrical parameters ϵ and σ of the mixture used will be assumed to be frequency independent in the band 1–10 GHz. The assumed values will be $\epsilon_r = 9.3$ and $\sigma = 2.88$ S/m, which correspond to measurements at 9.3 GHz.

The above assumption may introduce some discrepancy between experimental and theoretical results in the low-frequency end of the band since in rocks and related materials it has been found that, in general, conductivity increases and the dielectric constant decreases with frequency, with much lower variations for ϵ [6].

Numerical values for the attenuation constant α and the phase constant β, obtained from (2) and (3), are plotted in Figs. 7 and 8 where the experimental values (represented by crosses) are also included. There is an excellent agreement between the experimental and the theoretical results which supports the validity of the approximate theoretical model and makes clear that the low-order hybrid modes propagating in this case may be considered as perturbations of the TE_{10}, TE_{12}, and TE_{30} modes in a perfectly conducting guide of cross section $a \times b$. (Another, but much more difficult, procedure for mode identification could be to measure the field distributions in the transverse section of the tunnel and compare with theoretical expressions, such as given by Emslie *et al.* [8]; however, this was deemed unnecessary because of the good agreement shown in Fig. 8.)

As shown in Fig. 7, the excited mode with the lowest attenuation is the perturbed TE_{10}. Its attenuation constant monotonically decreases with increasing frequency. The detection of higher order modes (perturbed TE_{12} and TE_{30}) propagating simultaneously with the TE_{10} was possible at frequencies above the corresponding cutoff frequencies in a perfectly conducting tunnel, although their attenuation constant was high.

It is noteworthy that at the high end of the frequency band considered, the mode detected with highest amplitude was the perturbed TE_{30} in spite of its high attenuation compared to that of the TE_{10} mode. This can be justified recalling that the measured relative amplitudes included in Table I are influenced by the mode-coupling efficiency of the transmitting and receiving probes. (In a metallic rectangular waveguide, the amplitude ratio between any two TE_{nm} modes excited by a centered electric probe depends on the probe height, the field distribution, and the wave impedance of the corresponding mode; but in the special case of TE_{n0} modes, where there is no field variation along the probe axis, the amplitude ratio of the modes is given by the ratio of the corresponding wave impedances [9].)

The circles in Fig. 7 represent measured attenuation values of natural propagation in the Lanaye tunnel, scaled by a factor of 50, showing similarity to the results obtained in the model, especially in the high end of the band where refraction loss predominates over ohmic loss, and therefore the influence of a not exactly scaled conductivity diminishes.

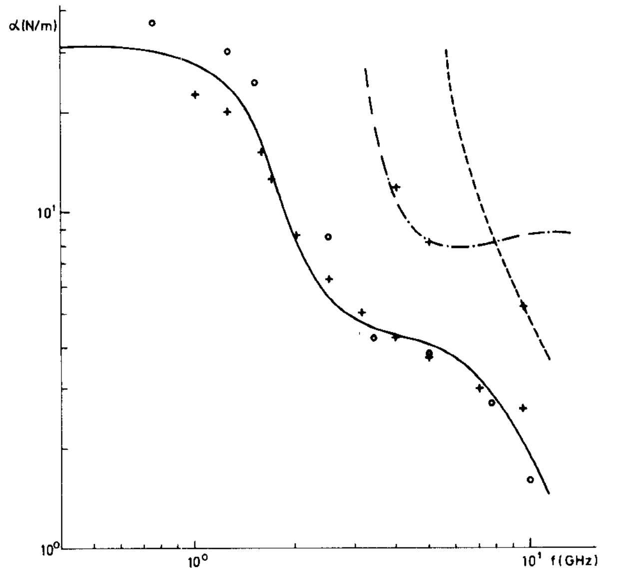

Fig. 7. Attenuation constant against frequency. —— TE_{10}, -·-·- TE_{12}, ----- TE_{30}, + Exp., ∘ Lanaye.

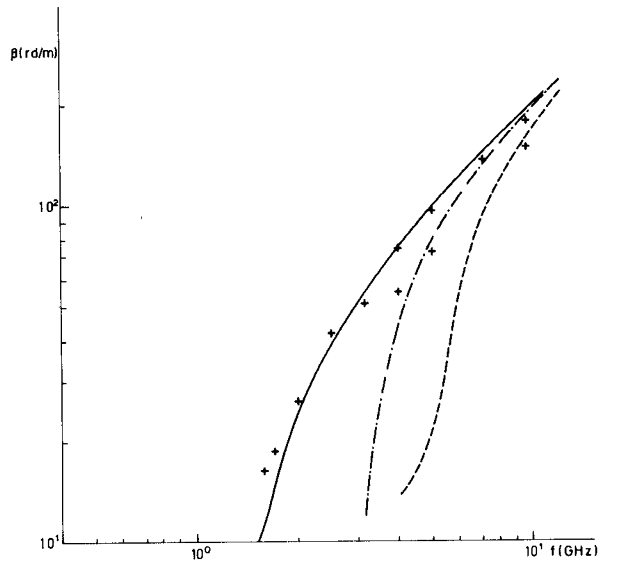

Fig. 8. Phase constant against frequency. —— TE_{10}, -·-·- TE_{12}, ----- TE_{30}, + Exp.

VI. Conclusions

Microwave modeling of a rectangular tunnel with a mixture of sand, water, and salt has permitted the experimental investigation of some of the natural propagation characteristics in less time and at lower cost than in a real tunnel.

The results show considerable similarity to those from a full-size tunnel in Belgium, although its conductivity was not exactly scaled in the model. Also, the good agreement found between experimental and theoretical results for the propagation constant of the natural modes in the tunnel model confirm the validity of the theoretical approach used.

The model has contributed to the understanding of the propagation mechanism in rectangular tunnels, showing that at high frequencies higher order modes can be better excited than the dominant mode (perturbed TE_{10}) although the latter has a lower attenuation. This fact may produce an interference pattern with deep nulls in the amplitude distribution along the tunnel which may preclude the use of too high frequencies for mobile radio communications using the tunnel as a guide.

The modeling technique used here has provided reliable data for electromagnetic wave propagation in rectangular tunnels. The versatility of the wet-sand mixture in simulating tunnel walls (ϵ, σ can be easily varied by changing the relative percentages of the mixture constituents) suggests that this technique may be successfully used to investigate the influence of different electrical and geometrical characteristics of tunnels (such as cross section, rugosity, curvatures, intersections, obstructions, and conductors) on propagation.

Appendix
Analysis of Two-Mode Propagation

We shall consider two modes $E_1(z)$ and $E_2(z)$ propagating in the z^+ direction with detected amplitudes E_1', E_2' at the feed position $z = 0$ and propagation constants γ_1, γ_2.

The total field, neglecting reflections, is therefore given by

$$E_T(z) = E_1' e^{-\alpha_1 z - j\beta_1 z} + E_2' e^{-\alpha_2 z - j(\beta_2 z - \psi)} = |E_T(z)| e^{j\phi(z)} \quad \text{(A1)}$$

where ψ is the phase difference between the two modes at $z = 0$.

The amplitude of $E_T(z)$ is

$$|E_T(z)| = \left\{ E_1'^2 e^{-2\alpha_1 z} + E_1'^2 e^{-2\alpha_2 z} + 2E_1'E_2' e^{-(\alpha_1+\alpha_2)z} \cos\left[(\beta_1 - \beta_2)z + \psi\right]\right\}^{1/2}. \quad \text{(A2)}$$

Equation (A2) represents an interference pattern whose beat wavelength is given by

$$\lambda_b = 2\pi/(\beta_1 - \beta_2). \quad \text{(A3)}$$

The maxima and minima of the beat pattern will occur at positions z_i such that $(\beta_1 - \beta_2)z_i + \psi$ is equal to $2n\pi$ and $(2n+1)\pi$, respectively ($n = 0,1,2,\cdots$).

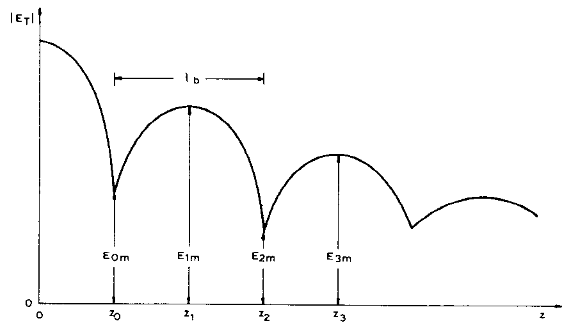

Fig. 9. Two-mode interference pattern.

Defining the amplitudes $E_{0m}(z_0)$, $E_{1m}(z_1)$, $E_{2m}(z_2)$, and $E_{3m}(z_3)$ as in Fig. 9, we have

$$E_{0m} = E_1' e^{-\alpha_1(z_1 - \Delta)} - E_2' e^{-\alpha_2(z_1 - \Delta)} \quad \text{(A4)}$$

$$E_{1m} = E_1' e^{-\alpha_1 z_1} + E_2' e^{-\alpha_2 z_1} \quad \text{(A5)}$$

$$E_{2m} = E_1' e^{-\alpha_1(z_1 + \Delta)} - E_2' e^{-\alpha_2(z_1 + \Delta)} \quad \text{(A6)}$$

$$E_{3m} = E_1' e^{-\alpha_1(z_1 + 2\Delta)} + E_2' e^{-\alpha_2(z_1 + 2\Delta)} \quad \text{(A7)}$$

where $\Delta = \lambda_b/2$.

From (A4) to (A7) the following equation for α_2 may be obtained:

$$\frac{e_1}{e_1e_3 - e_2^2}v^{-3} + \left(\frac{1}{e_2 - e_1^2} + \frac{2e_2}{e_1e_3 - e_2^2}\right)v^{-2} + \left(\frac{2e_1}{e_2 - e_1^2} + \frac{e_3}{e_1e_3 - e_2^2}\right)v^{-1} + \frac{e_2}{e_2 - e_1^2} = 0 \quad \text{(A8)}$$

where $v = e^{\alpha_2 \Delta}$ and

$$e_i = \frac{E_{im}}{E_{0m}} \qquad (i = 1,2,3).$$

Equation (A8) can be factorized as follows:

$$\left(\frac{1}{e_1e_3 - e_2^2}v^{-2} + \frac{e_3 - e_1e_2}{(e_1e_3 - e_2^2)(e_2 - e_1^2)}v^{-1} + \frac{1}{e_2 - e_1^2}\right)(e_1v^{-1} + e_2) = 0. \quad \text{(A9)}$$

Roots for v with physical meaning can only be obtained from the quadratic factor of (A9)

$$(e_2 - e_1^2)v^{-2} + (e_3 - e_1e_2)v^{-1} + e_1e_3 - e_2^2 = 0. \quad \text{(A10)}$$

A real and positive solution of (A10) permits one to calculate α_2

$$\alpha_2 = \frac{1}{\Delta}\ln v. \quad \text{(A11)}$$

The rest of the field parameters are given by

$$\alpha_1 = \frac{1}{\Delta}\ln\frac{1 + Kv}{e_1 - K} \quad \text{(A12)}$$

$$E_2'/E_{0m} = Ke^{\alpha_2 z_1} \quad \text{(A13)}$$

$$E_1'/E_{0m} = (e_1 - K)e^{\alpha_1 z_1} \quad \text{(A14)}$$

where

$$K = \left(e_1^2 - e_2\right) / \left(\frac{1}{v} + ve_2 + 2e_1\right). \qquad \text{(A15)}$$

If it is assumed that the phase constant of one of the modes is known from the phase distribution, the phase constant of the other mode is obtained from (A3).

The phase shift ψ may be obtained from the position of one of the minima (z_{2n}) in the experimental beat pattern

$$\left\{ \psi = \pi\left(2n + 1 - \frac{2z_{2n}}{\lambda_b}\right) \qquad n = 0,1,2,\cdots \right\}.$$

In case of uncertainty in the magnitude of some minima in the measured interference pattern, it is possible to use a similar procedure for identifying the unknown field parameters using only the magnitude and position of maxima or other suitable combinations of both maxima and minima.

Acknowledgment

The authors wish to thank the reviewers for their valuable comments and suggestions.

References

[1] P. S. Hall, B. Chambers, and P. A. McInnes, "Microwave modelling of H. F. Yagi antennas over imperfectly-conducting ground," *Proc. Inst. Elec. Eng.*, vol. 125, pp. 261–266, Apr. 1978.

[2] B. Jacard and G. Gómez, "Microwave modelling of H. F. antennas over lossy earth," in *1981 IEEE MTT-S Int. Microwave Symp. Dig.*, (Los Angeles, CA), June 15–19, 1981, pp. 90–92.

[3] B. Jacard, A. Valenzuela, and O. Maldonado, "Parallel planes approximation for propagation in rectangular tunnels," *Electron. Lett.*, vol. 18, pp. 1011–1012, 11 th. Nov. 11, 1982.

[4] S. F. Mahmoud and J. R. Wait, "Geometrical optical approach for electromagnetic wave propagation in rectangular mine tunnels," *Radio Sci.*, vol. 9, pp. 1147–1158, Dec. 1974.

[5] S. Ramo, J. R. Whinnery, and T. Van Duzer, *Fields and Waves in Communication Electronics.* New York: Wiley, 1965, ch. 7, pp. 379–382.

[6] P. Delogne, *Leaky Feeders and Subsurface Radio Communications*, Stevenage, U.K.: Peter Peregrinus, 1982, ch. 1 & 2.

[7] L. Deryck, "Natural propagation of electromagnetic waves in tunnels," *IEEE Trans. Veh. Technol.*, vol. VT-27, pp. 145–150, Aug. 1978.

[8] A. G. Emslie, R. L. Lagace, and P. F. Strong, "Theory of the propagation of VHF radio waves in coal mine tunnels," *IEEE Trans. Antennas Propagat.*, vol. AP-23, pp. 192–205, Mar. 1975.

[9] R. E. Collin, *Foundations for Microwave Engineering.* New York: McGraw-Hill, 1966, ch. 4, pp. 183–187.

Benjamin Jacard was born in Santiago, Chile, on October 8, 1944. He received the degree of Civil Electrical Engineer in 1971 from the University of Chile, where he has been a member of the academic staff of the Department of Electrical Engineering since 1969.

In 1972 and 1973, he carried out postgraduate studies in telecommunications at Imperial College, London, and in 1983, he received the Ph.D. degree in electrical engineering from the University of London, England. His main research interests are in electromagnetic wave propagation, radio noise, antennas, and radio communications in tunnels.

Oscar Maldonado was born in Chillán, Chile, on March 27, 1955. He received the Civil Electrical Engineer and M.S.E.E. degrees from the University of Chile in 1984 with specialization in telecommunications and digital systems.

At present, he is a part-time Research Assistant in the Department of Electrical Engineering, University of Chile, working on waveguide theory and electromagnetic wave propagation in tunnels.